

Implementing directional reflectance in a colour managed workflow

Tanzima Habib, Phil Green and Aditya Sole, Norwegian University of Science and Technology, Gjøvik, Norway.

Abstract

This paper implements an appearance rendering workflow using the iccMAX architecture with the aim of reproducing the directional appearance of surface colours on a display. In previous work, the prints were measured bidirectionally using an image-based measurement setup, and the bidirectional reflectance distribution function of the materials was estimated using the well-established Ward reflectance model. This function was applied in a colour managed workflow using the ICC.2 architecture to render the appearance of the prints on a display. The seven used as samples to the renderings.

Introduction

Colour management is increasingly concerned with the rendering of appearance rather than solely colorimetry. While 3D rendering softwares like Mitsuba renderer is able to apply sophisticated models to generate realistic simulations, there is a need to integrate appearance reproduction into existing colour management frameworks that can be implemented in production and process control.

Modeling the appearance of a material/object surface should take into account the directions of incident light and viewing, together with the optical properties of the material. A reflectance model such as Cook-Torrance or an empirical Ward model is commonly used in computer graphic to model material reflectance properties and estimate the bidirectional reflectance distribution function (BRDF) [1]. Reflectance models can be classified into physical or phenomenological models. Physical models use optics and physics to define the function using the micro facet theory, while phenomenological models use analytical models to fit measured data and estimate reflectance [1].

A series of directional measurements can be used to optimize reflectance model coefficients which can then be used to estimate material BRDF at a given incident and viewing direction. Bi-directional reflectance can be measured with a goniospectrophotometer but this can be relatively time consuming [2]. To overcome this limitation, image-based measurement setups have been proposed and used [2-4]. Marschner et. al. [3] demonstrates such a measurement setup to measure a variety of different samples like paints, and human skin. A similar setup was used by Sole et. al. [5,6] to measure packaging print materials and estimate material BRDF by optimizing the coefficients of the Cook-Torrance [7] and the isotropic Ward [8] models. In [5], a printed sample that is wrapped around a cylinder of known radius is illuminated using a point light source and the resulting radiance from the curved sample is measured using an RGB camera as detector. Figure 1 shows the schematic of the measurement setup used by Sole et. al [5, 6].

The measurements thus obtained were used to optimize reflectance model coefficients to estimate the full BRDF of the measured samples [2, 6]. These optimized reflectance model coefficients can be used to obtain a rendering of the materials at different illumination and viewing directions.

A software renderer such as Mitsuba [10] can apply different reflectance models to generate realistic simulations

either spectrally or in the sRGB domain. Integrating the renderer into existing colour management frameworks however can be a challenge. The ICC.2 (iccMAX) architecture [16] recently introduced by the International Color Consortium (ICC) incorporates a stack-based scripting language that makes it possible to encode a functional transform such as BRDF [11] within the profile.

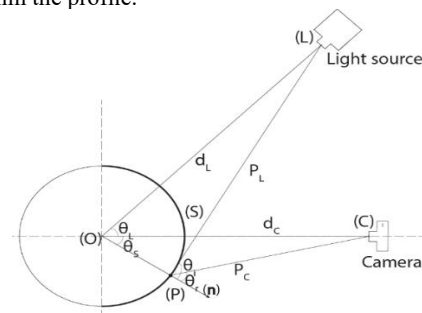


Figure 1. Image-based measurement setup [9].

In this paper, we use the BRDF coefficients calculated by Sole et. al. to optimize the isotropic Ward reflectance model. The coefficients were used as input data to the Ward model encoded in an iccMAX profile, which was then used to compute the colorimetry of a sample at different incident and viewing directions.

The objectives of the work presented in paper are:

1. to show a BRDF workflow is possible using iccMAX
2. to describe the implementation, performance and limitations of this workflow.

Image-based measurement

The samples used by Sole et al [5] were wax based inks printed on a matte coated white paper. They were pasted as strips on a circular structure with a marked angular ruler at the bottom as shown in Figure 1. Seven different colour samples namely, white, red, cyan, Pantone 10309C, magenta, Pantone 10213C and Pantone 10253C were printed using an OCE ColourWave 600 printer. These samples were measured using the image-based setup for 10 different illumination angles.

A tungsten illumination source was configured to approximate a point light source and the acquisition system was a Nikon D200 DSLR camera. The setup is shown in Figure 1 where the semi-circle S is the sample with radius R and center O . C is the position of the sensor (camera) placed normally from the mid-point of S at a distance d_C from O . L is the position of the light source at a distance d_L from O . The RGB intensities were taken from the raw images of the samples and the incident and reflected angles at each pixel (P) were calculated from the illumination angles (θ_i). (Full details can be found in Sole et. al. [5, 6]). The captured RGB intensities were converted to XYZ using the matrix M derived using the camera spectral sensitivity and the CIE 2° observer colour matching function [12].

The cyan and magenta samples were measured by Sole et. al. in [5] using a telespectroradiometer. These measurements provide a reference for analysis of the colorimetric output from the ICC profiles implemented in the present study.

Ward Model

As the samples are isotropic and planar, the isotropic Ward model was used to fit the measured reflectance data [5]. The equation for the isotropic and planar Ward model in this case is given by equation 1.

$$I_p(\theta_i; \theta_r) = \begin{bmatrix} I_{d_x} \\ I_{d_y} \\ I_{d_z} \end{bmatrix} = I_i \cos \theta_i \begin{bmatrix} R_{d_x} \\ R_{d_y} \\ R_{d_z} \end{bmatrix} \frac{1}{\pi} + \frac{k_s}{\sqrt{\cos \theta_i \cos \theta_r}} \frac{e^{-\tan^2 \delta / m^2}}{4\pi m^2} \quad (1)$$

where I_p is the camera colorimetric output (XYZ) at pixel P with incident angle θ_i and reflection angle θ_r . I_i is the incident light intensity, R_{dx} , R_{dy} and R_{dz} are the spectral diffuse reflectance components, k_s is the specular coefficient of the sample and $\cos \delta = \cos((\theta_i - \theta_r)/2)$ at pixel P [5].

Obtaining Ward Model coefficients

Reflection coefficients K_s , R_{dx} , R_{dy} and R_{dz} and m were fitted and optimized using the Nelder-Mead downhill simplex algorithm [13], with ΔE_{00} colour difference as the objective function [5].

Method

Workflow using iccMAX

A colour management framework applies a series of transforms in order to connect the source values to a destination colour space. In our case we wish to connect input data to a simulation of the directional appearance on a display. The connection from source device to XYZ, and from XYZ to display device, can be handled by device profiles, and so the core task addressed in this paper is to transform from XYZ representing the diffuse reflectance to an adjusted XYZ representing the appearance of the material once the angles of illumination and viewing have been taken into account.

Implementing the Ward model as described above is not possible within the colour management architecture defined by ICC.1 [14, 15] since this specifies a point-wise transform with a limited set of transform elements (curve, matrix and look-up table), and the Profile Connection Space (PCS) is defined to represent a matt, diffusely reflecting planar surface measured with a 0:45 geometry, and with a D50 illuminant.

ICC.2 [16], however, extends the ICC.1 architecture and provides a much richer support for colour management of other types of material and other geometries of measurement and viewing. Of relevance to our application, ICC.2 supports a wider range of transform elements, and fully directional illumination, measurement and viewing geometries.

ICC.2 incorporates the curve, matrix and LUT elements of ICC.1, but with fewer restrictions - unlike the fixed element sequence in ICC.1 transforms, they are defined more flexibly and can be applied in any number and order. ICC.2 also includes an option to use the 'calc' element, a script language which makes transforms fully programmable.

There are two basic modes in which BRDF data can be incorporated in an ICC.2 profile. Where it is expected that an external application, such as 3D rendering software, will perform the processing, *BRDFStruct* tags allow parameters for a BRDF model to be provided with the image data. Such an example was outlined by Vogh [17]. Where it is desired that the colour management module (CMM) use the device data and BRDF parameters to compute PCS values representing the appearance of a material at a given illumination and viewing angle, the required processing can be performed by the ICC.2 CMM. In this

case the transform must be defined by the profile creator, since while ICC.2 includes tags which allow angular geometry to be input with the image data, a conforming CMM is not required to have the ability to apply a BRDF model.

Although other ICC.2 transform elements could in principle be used to specify a BRDF transform, the most direct way to encode such a model is to use a calc element. A calc element is incorporated in a *multiProcessingElement*, which can be included in many of the ICC.2 transform types. BRDF Function tags, for example, provide four channels for specification of illumination and viewing angles in terms of both azimuth and elevation, in addition to the channels representing the source colour space. However, in our application we wish to define five optimized parameters for each colour for the Ward BRDF model, as described above, and rather than specify illumination and viewing angles for each pixel we only define a single set of angles for the image.

The *brdfBToA1Tag* provides additional channels for specification of illumination and viewing angles, but not for parameters as defined by the Ward model.

Other options for defining these parameters include:

- using an xCLR colour space, where x would be the number of source colour space channels plus four, in conjunction with an AToB1 tag.
- using a multiplex connection space (MCS) that supports the additional channels.

Since the model parameters identify the material rather than the colour, in this initial implementation we have chosen to use an MCS to connect input XYZ data and optimized coefficients with the visualization.

Multiplex Connection Space

Data representing multiple channels is passed into an MCS by a Multiplex Identification (MID) profile. Once in the MCS, the channels can be routed through different pathways depending on the requirements. A Multiplex Visualization (MVIS) profile can be used to connect the channels to a colorimetric or spectral PCS, performing any processing needed to convert to this PCS [18]. The *multiplexTypeArrayTags* is defined to assign channel names and is used to match channels in and out of the MCS, and check channel compliance to any subset requirements between profiles. The optional *multiplexDefaultValuesTag* defines default values for channels. A MID class profile uses an *AToM0* tag to provide the transform from device channel data to MCS channel data while MVIS class profile can use *MToS0* (spectral) or *MToB0* (colorimetric) tags to provide transform from MCS channel data to PCS channel data. Once the source and destination profiles are connected, the source MCS channels connect to the destination MCS channels with matching names [16]. The workflow of MID – MVIS connection with no subset requirements is used to encode the Ward model as shown in Figure 3. The Ward model is encoded in a *calculatorElements* tag as a main function [19].

In this workflow, the BRDF model optimized coefficients (R_{dx} , R_{dy} , R_{dz} , k_s and m) for each sample are passed through 'nc0005' input channels to the MID profile. These 5 input channels are passed to the MVIS profile through MCS connection. The desired viewing angles θ_i and θ_r are passed in at run-time as environment variables (*incident* and *reflection* respectively) to the MVIS profile, where the Ward model is encoded as in Eqn. 1 inside the calculator element tag of *MToA0* tag. The MVIS profile takes the 5 input channels, together with the environment variables for incident and viewing angles, and

applies the encoded Ward model to output PCS XYZ [19]. This workflow was implemented as follows:

1. A TIFF file is used to store per pixel the five BRDF coefficients R_{dx} , R_{dy} , R_{dz} , k_s and m .
2. A MID profile reads these channels from the TIFF file and passes them to the MCS.
3. An MVIS profile then takes the channels from the MCS and applies the BRDF ward model using the parameters pixelwise. Finally, a new TIFF file is created with the estimated XYZ values for the given incidence and viewing angles.

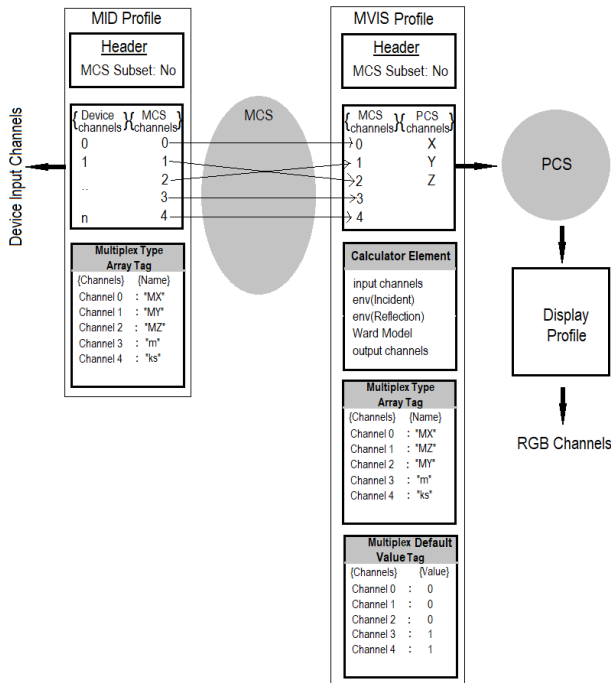


Figure 2. MID-MVIS to encode Ward Model workflow.

Custom PCS

The measured radiance of the source light used to illuminate the samples [5], after normalization, was (0.97, 1, 0.484). Since this is different from the standard D50 PCS used in ICC colour management, a *customToStandardPccTag* has to be defined with the tag signature 'c2sp' as a *multiProcessElementType*. This tag converts from the custom colorimetry to standard D50 colorimetry. The matrix to be included inside this tag is the chromatic adaptation transform matrix from custom white point as the source to D50 white point as the destination. Similarly, a *standardToCustomPccTag* using tag signature 's2cp', is required to define the inverse of this chromatic adaptation transform matrix. The linear Bradford chromatic adaptation transform was used to create the 3x3 transform matrix from custom source white point to D50, as recommended in the ICC specification. A *spectralViewingConditions* tag is also defined to include the spectral power distribution of the illuminant, colour matching functions (CMFs) of the observer and the lighting levels of the surround [16].

Results and discussion

The profiles created were applied to TIFF files containing BRDF parameters to obtain XYZ values for different pairs of (incidence, reflection) angles, for each sample. A summary of

the results is given in Table 1, a selection of reflectance functions for cyan and magenta are compared with measured values. In Figures 3-8, and a visualization of the results is shown in Figures 9-12.

Performance of profiles relative to Ward model predictions

Table 1. shows the ΔE_{2000} calculated between the estimated XYZ obtained by applying the ICC profile and the estimated XYZ obtained by Sole et. al. [5] and ΔE_{2000} calculated between the estimated XYZ obtained by applying the ICC profile and the estimated XYZ obtained by isotropic Ward model implemented in MATLAB for cyan sample with incidence and reflection angles as $(40^\circ, -10^\circ)$, $(40^\circ, 0^\circ)$, $(40^\circ, 10^\circ)$ and $(40^\circ, 30^\circ)$. In this paper, reflection angle is synonymous to viewing direction. The ΔE_{2000} calculated between MATLAB is negligible while the ΔE_{2000} with Sole et.al. is less than 1.0.

(θ_i, θ_r)	ΔE_{2000} (a)	ΔE_{2000} (b)
$(40^\circ, -10^\circ)$	0.6407	0.0011
$(40^\circ, 0^\circ)$	0.6644	0.0010
$(40^\circ, 10^\circ)$	0.7157	5.8370e-04
$(40^\circ, 30^\circ)$	0.8636	1.2928e-04

Table 1. (a) ΔE_{2000} between estimated XYZ obtained by Sole. et. al. and estimated XYZ obtained using ICC profiles and (b) ΔE_{2000} between estimated XYZ obtained using MATLAB and estimated XYZ obtained using ICC profiles for cyan sample with incidence and reflection angles as $(40^\circ, -10^\circ)$, $(40^\circ, 0^\circ)$, $(40^\circ, 10^\circ)$ and $(40^\circ, 30^\circ)$. Performance of Ward model encoded as ICC profile in predicting directional measurements

In Figure 3, Figure 4 and Figure 5 for incidence angles 30° , 45° and 60° respectively of the cyan sample, the Y values of the estimated XYZ using the MVIS profile, estimated XYZ adapted to D50, D65 and A illuminants and the reference XYZ with D50 white point are plotted for reflection angles ranging from 80° to -80° in steps of 5° . The estimated Y curves predict the specular lobe on the left of the y-axis at the correct reflection angles when compared to the reference Y curve. Although in Figures 4 and 5, as the incidence angle increases the Y values near the specular lobe are somewhat underestimated.

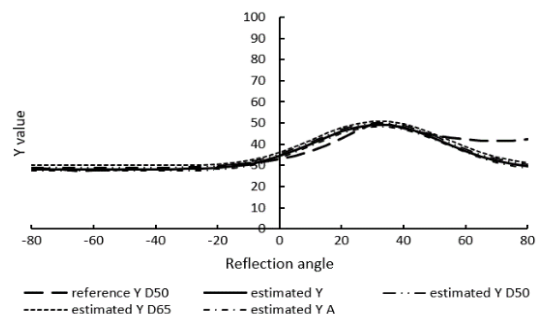


Figure 3. For cyan sample and incidence angle 30° , the reference Y, estimated Y, estimated Y adapted to D50, adapted to D65 and adapted to A values are plotted in the y-axis and reflection angles from -80° to 80° in the x-axis.

Similarly, in Figures 6-8 for the magenta sample and incidence angles 30° , 45° and 60° respectively, the Y values of the estimated XYZ using MVIS profile, estimated XYZ adapted to D50, D65 and A illuminants and the reference XYZ with D50 white point are plotted for reflection angles ranging from 80° to -80° in steps of 5° . Although in Figure 6 the Y values near the

specular lobe are overestimated, in Figures 7 and 8 as the incidence angle increases the Y values near the specular lobe are largely underestimated.

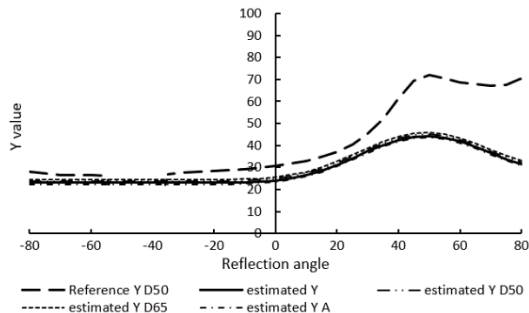


Figure 4. For cyan sample and incidence angle 45°, the reference Y, estimated Y, estimated Y adapted to D50, adapted to D65 and adapted to A values are plotted in the y-axis and reflection angles from -80° to 80° in the x-axis.

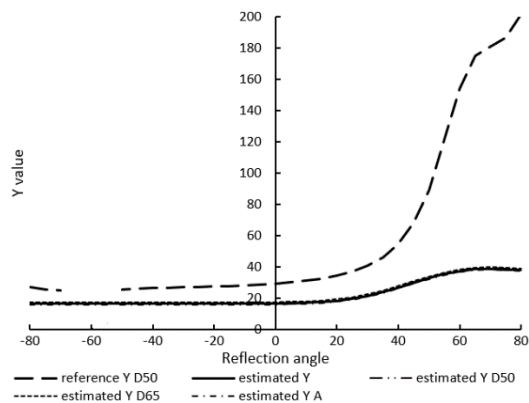


Figure 5. For cyan sample and incidence angle 60°, the reference Y, estimated Y, estimated Y adapted to D50, adapted to D65 and adapted to A values are plotted in the y-axis and reflection angles from -80° to 80° in the x-axis.

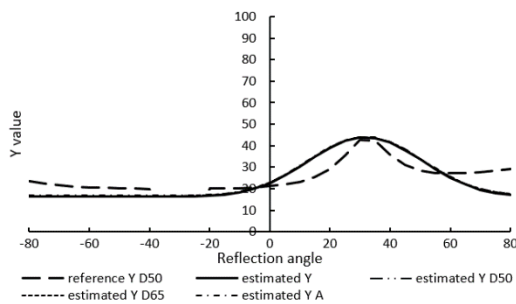


Figure 6. For magenta sample and incidence angle 30°, the reference Y, estimated Y, estimated Y adapted to D50, adapted to D65 and adapted to A values are plotted in the y-axis and reflection angles from -80° to 80° in the x-axis.

Figures 9 -12 are sRGB images of estimated XYZ at incidence angles -30°, 0°, 45° and 60° for reflection angles from [-80°,80°] in steps of 5° of cyan, magenta, Pantone 10309C and Pantone 10213C samples respectively, used by Sole et al [5]. These sRGB images are created after adapting the estimated XYZ values to D65 and then converting them to sRGB. From the images the increased reflectance of the specular lobe can be seen, and as the difference between the incidence angle and the normal at 0° increases, the shades become darker.

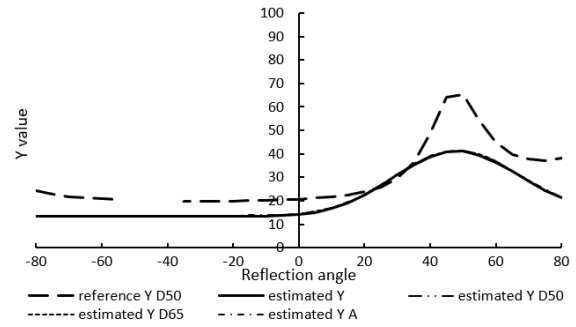


Figure 7. For magenta sample and incidence angle 45°, the reference Y, estimated Y, estimated Y adapted to D50, adapted to D65 and adapted to A values are plotted in the y-axis and reflection angles from -80° to 80° in the x-axis.

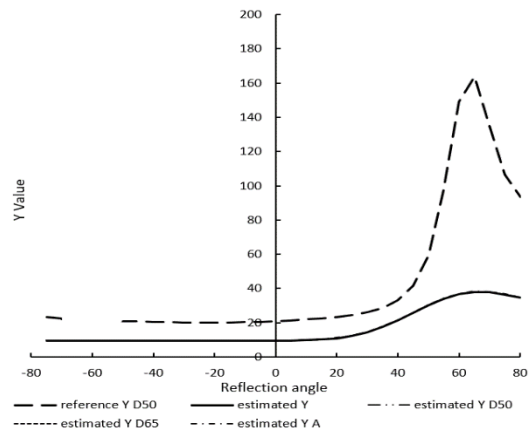


Figure 8. For magenta sample and incidence angle 60°, the reference Y, estimated Y, estimated Y adapted to D50, adapted to D65 and adapted to A values are plotted in the y-axis and reflection angles from -80° to 80° in the x-axis.

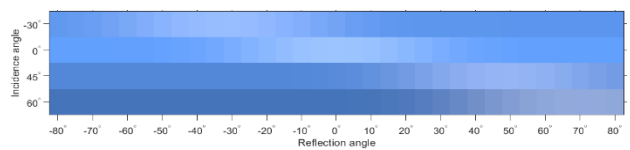


Figure 9. sRGB image of estimated XYZ at incidence angles -30°, 0°, 45° and 60° for reflection angles from [-80°,80°] in steps of 5° of cyan sample.

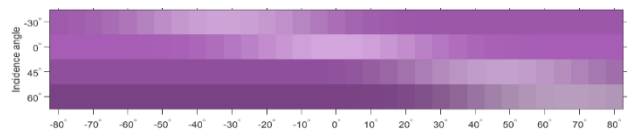


Figure 10. sRGB image of estimated XYZ at incidence angles -30°, 0°, 45° and 60° for reflection angles from [-80°,80°] in steps of 5° of magenta sample.

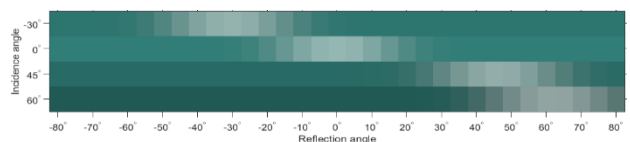


Figure 11. sRGB image of estimated XYZ at incidence angles -30°, 0°, 45° and 60° for reflection angles from [-80°,80°] in steps of 5° of cyan sample.

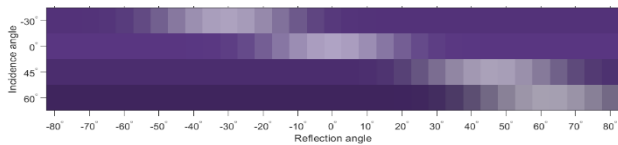


Figure 12. sRGB image of estimated XYZ at incidence angles -30° , 0° , 45° and 60° for reflection angles from $[-80^\circ, 80^\circ]$ in steps of 5° of cyan sample.

The results show that the Ward BRDF model behaves as expected with a smooth Gaussian output when encoded in an ICC profile. These results also show that the performance of an ICC profile encoded BRDF rendering is equivalent to rendering with other computational tools.

Conclusions

Based on a method to obtain fast and low-cost multi angle measurements [5], this paper demonstrates how to extract the BRDF parameters and perform appearance rendering through ICC profiles for any incident light angle and viewing angle pair. Using the MCS connection an efficient reflection model workflow was implemented to render final colorimetric (of device) values for the seven samples with the incident and the reflection angles passed at runtime. The BRDF parameters were passed pixelwise using a TIFF file. This colour-managed workflow gives identical results to the Ward model implementation in Matlab for the equivalent adapted colorimetry, and agrees well with previous results [5].

The Ward model as implemented accurately predicts the reflection angle of the specular lobe. While it performs well in estimating the measured reflectance at different angles of some of the samples, in others it performs less well. This may be due to a failure to take the angular reflectance properties fully into account in deriving the optimized model parameters.

In the future, other reflectance models beyond the isotropic Ward model should be tested. These preliminary results have highlighted some of the limitations and the improvements required. Different metrics could be chosen for optimization of BRDF parameters, with weighting for different appearance parameters such as hue, lightness or chroma, if required. Other BRDF measurement setup should be compared to the one discussed here. For non-planar surfaces the workflow could incorporate incidence and/or viewing angles per pixel in addition to model parameters.

Acknowledgement

This project has received funding from the European Union's Horizon 2020 research and innovation programme under the Marie Skłodowska-Curie grant agreement No. 814158.

References

- [1] D. Guarnera, G. C. Guarnera, A. Ghosh, C. Denk, and M. Glencross, "BRDF representation and acquisition." In Computer Graphics Forum, 2016, vol. 35, no. 2: Wiley Online Library, pp. 625-650
- [2] A. Sole, I. Farup, P. Nussbaum, and S. Tominaga, "Bidirectional Reflectance Measurement and Reflection Model Fitting of Complex Materials Using an Image-Based Measurement Setup."

- Journal of Imaging, vol. 4, no. 11, p. 136, Nov 2018, doi: ARTN 136.
- [3] S. R. Marschner, S. H. Westin, E. P. F. Lafortune, K. E. Torrance, and D. P. Greenberg, "Image-based BRDF measurement including human skin." In 10th Eurographics Workshop on Rendering, pp. 139 – 152, (1999).
- [4] A. Ngan, F. Durand, and W. Matusik, "Experimental analysis of BRDF models." Rendering Techniques, vol. 2005, no. 16th, p. 2, 2005
- [5] A. S. Sole, I. Farup and S. Tominaga. "An image-based multi-directional reflectance measurement setup for flexible objects. " In Measuring, Modeling, and Reproducing Material Appearance. International Society for Optics and Photonics. Vol. 9398, p. 93980J (2015).
- [6] A. Sole, I. Farup, P. B. Nussbaum., "Evaluating an image based multi-angle measurement setup using different reflection models. " Electronic Imaging, pg. 101-107. (2017).
- [7] R. L. Cook and K. E. Torrance, "A Reflectance Model for Computer Graphics". ACM Trans. Graph., vol. 1, no. 1, pp. 7-24, jan/ 1982. <http://doi.acm.org/10.1145/357290.357293>
- [8] G. J. Ward, "Measuring and Modeling Anisotropic Reflection." SIGGRAPH Comput. Graph., vol. 26, no. 2, pp. 265-272, jul/ 1992. [Online]. Available: <http://doi.acm.org/10.1145/142920.134078>
- [9] A. Sole, "Image-Based Bidirectional Reflectance Measurement of Non-Diffuse and Gonio-Chromatic Materials." ISBN 9788232642847. Doctoral thesis at Norwegian University of Science and Technology (2019:344), 2019
- [10] W. Jakob, "Mitsuba Physically Based Renderer." (2010). <http://www.mitsuba-renderer.org>.
- [11] M. Derhak, P. Green and T. Lianza "Introducing iccMAX – New Frontiers in Colour Management." Proc. SPIE 9395, Colour Imaging XX: Display, Processing, Hardcopy, and Applications, 93950L, (2015).
- [12] A. Sole, I. Farup, S. Tominaga, "Image based reflectance measurement based on camera spectral sensitivities." Electronic Imaging, pp. 1-8. (2016).
- [13] M. Smith, "A simplex method for function minimization." The Computer Journal., 7(4):308-13 (1965).
- [14] ICC.1:2010. "Image technology colour management — Architecture, profile format and data structure. " (2010).
- [15] ISO 15076-1:2010 "Image technology colour management - Architecture, profile format, and data structure. " (2010).
- [16] ICC.2:2018. Image technology colour management -- Extensions to architecture, profile format, and data structure, iccMAX. (2018).
- [17] J. Vogh, "3D Appearance Management using iccMAX. " ICC Meeting on Display and 3D Printing, Taipei (2016). http://www.color.org/events/taipei/7-3D_Appearance_Management_using_iccMAX.pdf
- [18] ICC, "iccMAX Reference Implementation. " <http://www.colour.org/iccmax/>, accessed January 2020
- [19] ICC, White Paper 45. "iccMAX Multiprocessing Element Calculator Programming. " (2019).

Author Biography

Tanzima Habib is a PhD scholar at NTNU. Currently, she is researching on appearance reproduction and colour management system for spectral and 2.5D printing.

Phil Green is Professor of Colour Imaging at the Colour and Visual Computing Laboratory, NTNU, Norway. He is also Technical Secretary of the International Colour Consortium.

Aditya Sole is working as a Project Leader at NTNU and has recently obtained his doctoral degree at the Department of Computer Science. His research interest is to develop and evaluate procedures for measuring the visual appearance of non-diffuse materials.